Math. Appl. 15(2)2026, 90–99

Chaotic Synchronization of Partial Differential Equations by Partial Driving: Framework and Selected Models

Berguellah Nour elhouda

Received: 05-03-2026 Accepted: 28-10-2026 Published:09-11-2026

Abstract: *We study chaotic synchronization between two copies of a spatially extended system governed by a partial differential equation (PDE) when the second copy, the slave, receives only partial information from the first, the master: measurements at a few points, or only the low-frequency modes. After setting up the general framework, we explain why dissipation makes the amount of information required finite, and we apply the idea to three models: the Kuramoto–Sivashinsky equation, the two-dimensional Navier–Stokes equations and the complex Ginzburg–Landau equation. Two numerical experiments, one on Kuramoto–Sivashinsky with point observations and one on a two-dimensional turbulent flow observed through its large scales, show how the error decays and how the density of observations decides whether synchronization occurs. We close with applications, mainly data assimilation for weather and ocean forecasting, and with the limitations of the approach.*

Introduction

In 1990 Pecora and Carroll showed that a chaotic system can be split into a drive subsystem and a response subsystem, and that the response converges to the drive trajectory from different initial conditions as long as all its conditional Lyapunov exponents are negative [12, 13]. They worked with ordinary differential equations (ODEs), where sending a single variable of the drive is enough.

For spatially extended systems the state space is infinite-dimensional, so the natural question is how much information the response needs. Dissipation supplies the answer. A dissipative system evolves toward a finite-dimensional attractor, and its state is fixed by a finite number of determining modes. The subject developed along two lines: nonlinear dynamics (Kocarev, Parlitz, Junge), which studied synchronization numerically and experimentally, and mathematical analysis (Foias and Prodi, then Olson and Titi), which proved rigorous results. In this article we put the two viewpoints side by side. A general introduction to synchronization can be found in [2].

Superior School of Accounting and Finance of Constantine, Algeria
Applied Mathematics and Modeling Laboratory, Constantine 1, Algeria
Email: nberguellah@escf-constantine.dz

Keywords: Chaotic synchronization, Partial driving, Partial differential equations, Determining modes, Data assimilation.

Mathematical Framework

Master and slave systems

Let the master be a dissipative evolution equation

$$u_t = F(u) \tag{1}$$

with a finite-dimensional global attractor. The slave obeys the same equation with an added feedback term that uses only partial information:

$$v_t = F(v) - \mu I_h(v-u). \tag{2}$$

Here μ > 0 is the coupling strength and Ih is an interpolation (or projection) operator that returns only the available data and satisfies an estimate of the form

$$\|\varphi - I_h\varphi\| \le c_0 h \|\varphi_x\|. \tag{3}$$

The parameter h is the observation resolution: the distance between measurement points, or h ~ 1/N when Ih projects onto the first N Fourier modes. The error w = v − u satisfies

$$w_t = F(v) - F(u) - \mu I_h w, \tag{4}$$

and synchronization means ‖ w(t) ‖ → 0 as t → ∞, usually at an exponential rate.

Relation to Pecora–Carroll driving

In the Pecora–Carroll scheme a variable of the response is replaced outright by the corresponding variable of the drive. Here the coupling is a gradual feedback instead. If Ih is the projection onto low modes, letting μ → ∞ replaces those modes by the master's and recovers the classical scheme as a limiting case.

Determining modes

Foias and Prodi [3] proved that if two solutions of the 2D Navier–Stokes equations converge in their first N modes, then they converge completely. Olson and Titi [4] later cast the same idea as a feedback scheme of the form (2). This is the theoretical basis of partial synchronization: dissipation damps the high modes, which end up slaved to the low ones. The number N that suffices depends on the Grashof number for Navier–Stokes and, more generally, on the dimension of the attractor.

Selected Models

The Kuramoto–Sivashinsky equation

$$u_t + u_{xx} + u_{xxxx} + u\,u_x = 0. \tag{5}$$

In one space dimension this equation has a linear instability at intermediate wavelengths and strong dissipation at short wavelengths through the term uxxxx. The result is spatiotemporal chaos on a finite-dimensional attractor whose dimension grows with the length of the domain.

Write the slave in the form (2) and test the error equation against w; the nonlinear term then reduces to ½∫ ux w2 dx, which gives the identity

$$\frac{1}{2}\frac{d}{dt}\|w\|^2 + \|w_{xx}\|^2 - \|w_x\|^2 + \frac{1}{2}\int u_x w^2\,dx = -\mu\,(I_h w, w). \tag{6}$$

We write (Ih w, w) = ‖ w ‖ 2 − (w − Ih w, w), bound the term − ‖ wx ‖ 2 by interpolating between ‖ w ‖ and ‖ wxx ‖ , and use (3) for the interpolation error. This leads to an inequality of the form

$$\frac{d}{dt}\|w\|^2 \le -\big(2\mu - K(t)\big)\|w\|^2, \tag{7}$$

where K(t) is controlled by ‖ ux ‖ ∞ of the master and by terms coming from the interpolation error, which shrink as h decreases. If the time average of K stays below 2μ, Gronwall's inequality gives exponential decay of the error. Synchronization thus requires a strong enough coupling and a fine enough observation grid. This is the nudging method in the general form given by Azouani, Olson and Titi [1].

Numerical experiment 1: point observations of Kuramoto–Sivashinsky

Setup. We take a periodic domain of length L = 22 with 128 Fourier modes and fourth-order exponential time stepping (time step 0.05). The master is run for 100 time units first, so that it lies on its chaotic attractor, and the slave starts from an unrelated small random field. The master is observed at n equally spaced points; linear interpolation between them plays the role of Ih, and the coupling strength is μ = 10. Both equations are integrated together so that the feedback uses the master at the same instant.

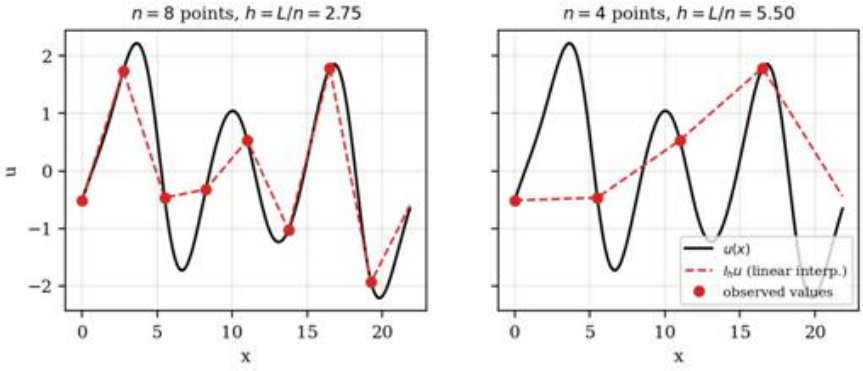


Figure 1: The observation operator in Experiment 1. A snapshot of the master u (black) is sampled at n equally spaced points (dots) and rebuilt by linear interpolation (dashed). With n = 8 the reconstruction follows the main oscillations; with n = 4 whole oscillations fall between the sample points.

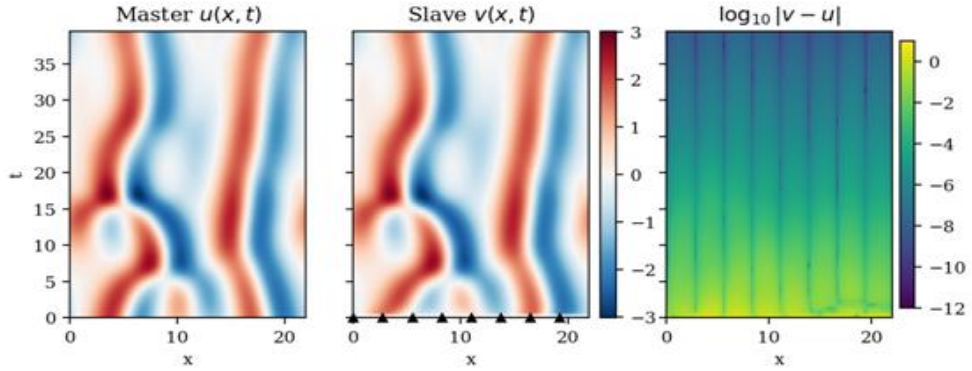


Figure 2: Space–time evolution of the master u (left), the slave v (middle) and the logarithm of their difference (right) with n = 8 observation points (triangles). The slave starts from a completely different state but becomes visually identical to the master, and the difference decays by many orders of magnitude.

Reading the results. With 8 or more points the error decays exponentially until it reaches round-off level. With 4 or 6 points it does not decay at all: when the grid is too coarse, synchronization is lost altogether. One way to read this is through the most unstable linear wavelength, $2\pi\sqrt{2} \approx 8.9$. Eight points give about three samples per such wavelength (h = 2.75), while six points give about 2.4. This agrees with a sampling-type threshold, but it is an empirical observation from these runs (see the parameter sweep below), not a proven criterion. With noisy observations the error cannot fall below a floor set by the noise: 1% noise in the data left an rms error near 2 × 10−3.

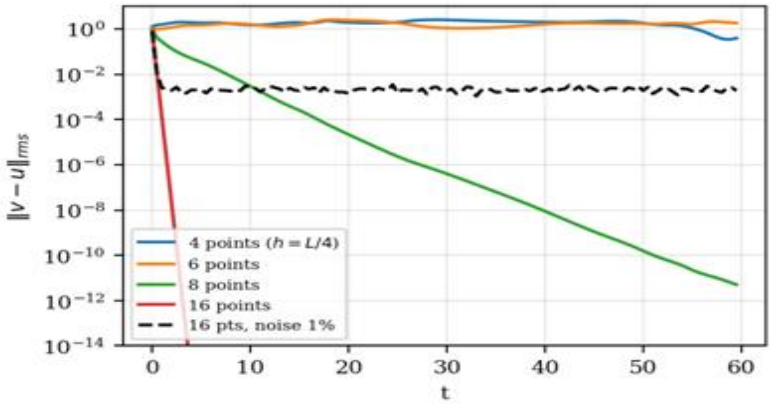


Figure 3: Root-mean-square error between slave and master versus time for different numbers of observation points (μ = 10), and for 16 points with 1% Gaussian noise added to the observations.

Table 1: Results of Experiment 1 (μ = 10).

Observation points	Spacing h = L/n	rms error of v − u at t = 60
4	5.5	does not decay (≈ 0.4)
6	3.7	does not decay (≈ 1.9)
8	2.75	5 × 10−12
16	1.4	≈ 10−16 (round-off)
16, with 1% noise	1.4	≈ 2 × 10−3 (plateau)

Parameter sweep. Figure 4 repeats the experiment for μ = 1, 3, 10 and 20. Over this range the outcome depends almost entirely on the number of points: n ≤ 6 never synchronizes, n = 7 decays slowly (error between about 3 × 10−5 and 10−3 at t ≈ 60), and n ≥ 8 reaches 10−10 or below. Raising μ from 1 to 20 does not reduce the number of points needed. This agrees with the structure of estimate (7): the interpolation error, controlled by h, has to be small enough before the coupling can act, and a stronger coupling cannot make up for missing information. As before, this is an observation for one realization of the master on one domain, not a theorem.

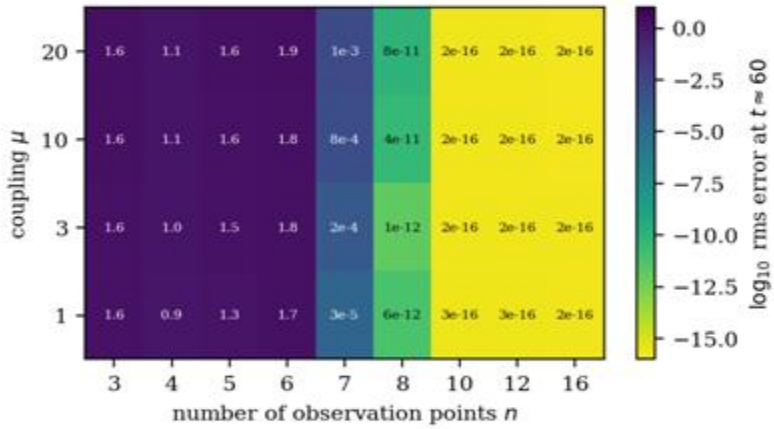


Figure 4: Parameter sweep for Experiment 1: rms error at t ≈ 60 (mean of the last 20 recorded values) as a function of the number of observation points n and the coupling μ.

The two-dimensional Navier–Stokes equations

$$u_t + (u \cdot \nabla)u - \nu \Delta u + \nabla p = f, \qquad \nabla \cdot u = 0. \tag{8}$$

We add the term −μ Ih(v − u) to the slave equation. When the error equation is tested against w, only b(w, u, w) survives from the nonlinear term; the other two contributions vanish by incompressibility. Ladyzhenskaya's inequality gives

$$|b(w,u,w)| \le c\,\|\nabla u\|\,\|w\|\,\|\nabla w\| \le \frac{\nu}{4}\|\nabla w\|^2 + \frac{c}{\nu}\|\nabla u\|^2\|w\|^2. \tag{9}$$

By (3), ‖ w − Ih w ‖ ≤ co h ‖ ∇ w ‖ , so if μ h2 is small compared with ν the interpolation term is absorbed by the viscous term. What remains is

$$\frac{d}{dt}\|w\|^2 \le \left(-\mu + \frac{c}{\nu}\|\nabla u\|^2\right)\|w\|^2,$$

and it is enough that μ exceeds the long-time average of ‖ ∇ u ‖ 2/ν, which is bounded in terms of the Grashof number. This is the continuous data assimilation theorem of Azouani, Olson and Titi [1]. It has since been extended to observations at discrete times (Hayden, Olson and Titi [7]) and to stochastically noisy data (Bessaih, Olson and Titi [6]).

Numerical experiment 2: a turbulent flow observed through its large scales

Setup. We use the vorticity form ωt + u·∇ω = νΔω + F on the doubly periodic square [0, 2π]2, with Kolmogorov forcing F = cos(4y), ν = 0.004, on a 64× 64 grid with 2/3 dealiasing and fourth-order Runge–Kutta time stepping (time step 0.01). The flow is chaotic: a perturbation of size 10−6 grew by about three orders of magnitude over 40 time units. The slave is an independent trajectory of the same flow started from a different initial condition (initial relative difference 1.26). The data are the Fourier modes of the master vorticity with |kx|, |ky| ≤ Nc, so Ih is a projection onto low modes, and μ = 20.

Table 2: Results of Experiment 2 (μ = 20).

Retained modes	Relative error at t = 30	Approx. decay rate
| kx|, | ky| ≤ 2 (25)	2.3 × 10−2	slow; still decreasing
| kx|, | ky| ≤ 4 (81)	1.2 × 10−5	≈ 0.36
| kx|, | ky| ≤ 8 (289)	7.6 × 10−12	≈ 0.8
| kx|, | ky| ≤ 12 (625)	3.6 × 10−17 (round-off)	limited by round-off

Reading the results. Every choice of Nc gives a decaying error, and the decay rate grows with the number of transmitted modes, as the determining-modes picture suggests: the more of the large scales are imposed, the faster the remaining scales lock on. Even 25 of the 4096 modes produce a steadily decreasing error, although slowly. With 81 modes the error falls by about five orders of magnitude within 30 time units, and the fine vortex filaments visible in the slave at t = 8 (Figure 5) were never observed; they are generated by the equations. These are single-run illustrations on a small grid. They show the mechanism but do not determine thresholds systematically.

Where the error goes first. Figure 7 splits the error by scale. Within one time unit the transmitted large scales have lost most of their error (below about 10−4), whereas the untransmitted small scales ($k \gtrsim 6$) still carry an error of order one. That error then drops by about two orders of magnitude by t = 8 and by about six by t = 20. The small scales are therefore not imposed; they lock on later, driven by the large scales through the nonlinearity, which is the mechanism behind the determining-modes theory.

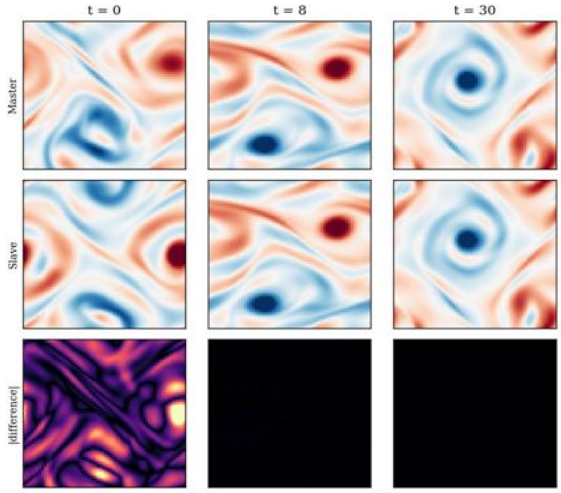


Figure 5: Vorticity of the master (top), of the slave (middle) and the absolute difference (bottom) at t = 0, 8 and 30, when only the 81 modes with |kx|, |ky| ≤ 4 are transmitted. The small scales of the slave are rebuilt by the dynamics itself.

The complex Ginzburg–Landau equation

$$A_t = A + (1 + i\alpha)A_{xx} - (1 + i\beta)|A|^2 A. \tag{10}$$

In the regime where the Benjamin–Feir–Newell instability holds and "defect turbulence" appears, the equation produces spatiotemporal chaos punctuated by points where the amplitude vanishes. Kocarev, Tasev and Parlitz [11] showed that systems of this type can be synchronized by partial driving, and Junge and Parlitz [9] showed that coupling localized at a few sites, or on part of the domain, is enough to synchronize both Ginzburg–Landau and Kuramoto–Sivashinsky equations. The

results are mainly numerical: the threshold depends on the spacing of the observation points relative to the chaotic correlation length, and there is no simple analytic formula comparable to the Navier–Stokes case.

We did not run a Ginzburg–Landau experiment for this article, but the protocol would be as follows. Choose (α, β) inside the Benjamin–Feir unstable region $1 + \alpha\beta < 0$, in a domain long enough for the dynamics to be chaotic. Run the master past its transient and couple the slave to it at M equally spaced sites, with a feedback term $-\mu(B - A)$ applied at those sites (or over a sub-interval of the domain). Then increase M, or the size of the coupling region, until the error $\| B - A \|$ decays. The smallest M for which this happens, compared with the correlation length of the chaotic state, gives the practical threshold.

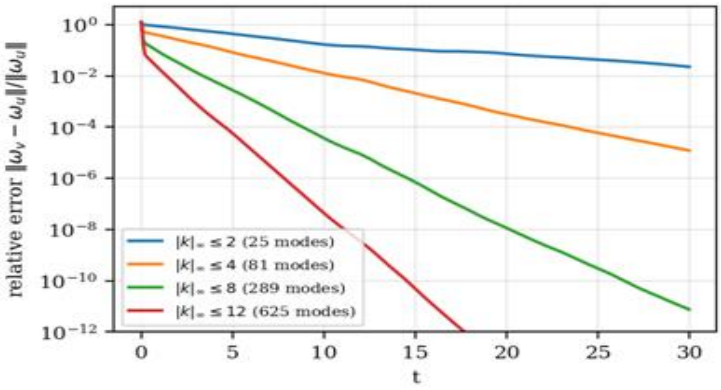


Figure 6: Relative vorticity error versus time for different numbers of transmitted modes (μ = 20).

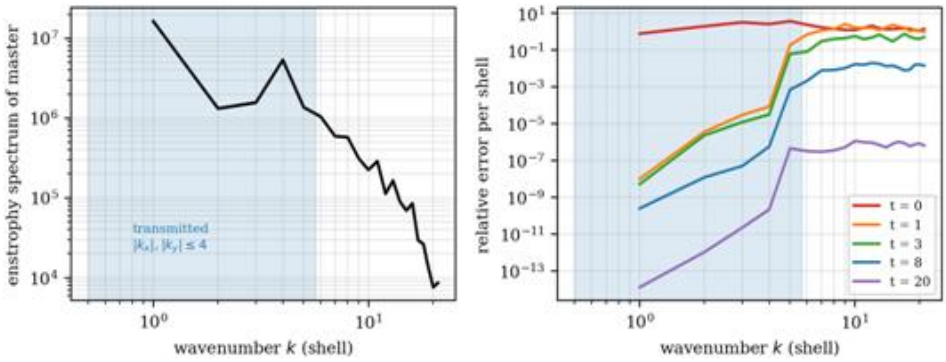


Figure 7: Left: enstrophy spectrum of the master summed over wavenumber shells (the peak at k = 4 is the forcing); the shaded band marks the transmitted modes. Right: error in each shell relative to the master at several times (Nc = 4, μ = 20).

Comparative summary

Table 3 compares the three models.

Table 3: Comparison of the three models.

Model	Dissipation	Information given to the slave	Synchronization condition (qualitative)
Kuramoto–Sivashinsky	Fourth-order term uxxxx	Values at grid points spaced by h	μ large enough and h small enough
2D Navier–Stokes	Viscosity ν	Large-scale modes or point values	$\mu \gtrsim \nu G^2$, $\mu h^2 \lesssim \nu$ (G: Grashof number)
Complex Ginzburg–Landau	Diffusive term (1 + iα)Axx	Values at points or on part of the domain	Point density vs. correlation length (numerical)

Numerical and methodological considerations

Time stepping. The coupling term $-\mu\, I h(v - u)$ becomes stiff when μ is large, so it is treated implicitly or with exponential integrators; otherwise the time step is restricted.

Measuring synchronization. Plot $\| w(t) \|$ on a logarithmic scale. A straight line indicates exponential decay, and its slope gives the synchronization rate.

Choice of μ. If μ is too small the coupling is insufficient; if it is too large it forces a small time step and amplifies measurement noise.

Parameter mismatch. When the model parameters differ between master and slave, the error does not vanish but stays bounded, typically by an amount proportional to the mismatch. This is a form of generalized synchronization (Kocarev and Parlitz [10]).

Noise. The error stays bounded by the noise level times a factor that depends on the coupling strength.

Applications

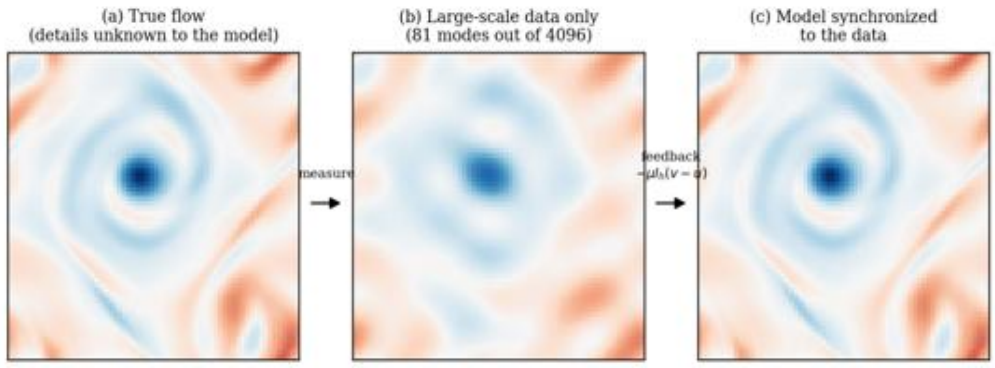


Figure 8: The idea behind data assimilation by synchronization, illustrated with the flow of Experiment 2: the model receives only the large-scale part of the true state (b), yet after feedback it reproduces the fine structure of the truth (c). This is a conceptual illustration, not an operational forecasting system.

Weather and ocean forecasting

Observations of the atmosphere and oceans come from stations, buoys, balloons and satellites, which sample the state sparsely and imperfectly. Relaxing a numerical model toward the observations (nudging, or Newtonian relaxation) has long been used in meteorology. The results above give this practice a rigorous basis

in model problems: with enough coupling and observation density the model state converges to the true state, and errors in the unobserved small scales are damped by the dynamics.

Downscaling

Downscaling is a related use: coarse-resolution measurements are used to recover fine-scale fields. Altaf and coauthors [14] applied continuous data assimilation in this spirit to the two-dimensional Bénard convection equations, reconstructing fine temperature and velocity fields from coarse data. Figure 5 shows the same principle for a flow.

Flow reconstruction from sparse sensors

In engineering, turbulent flows are often measured with a few probes or low-resolution images. The same feedback loop can estimate the full field from such data when a reliable model is available. Gesho, Olson and Titi [15] studied the algorithm numerically for the two-dimensional Navier–Stokes equations, including how performance depends on resolution and coupling strength.

Secure communication

Chaotic masking (Cuomo and Oppenheim [8]) hides a message in a chaotic carrier, and the receiver, a synchronized slave, subtracts the carrier. Its security has been challenged by methods that extract the message from the transmitted signal (for example Pérez and Cerdeira [5]), so it is best regarded as a historical application rather than a secure technique.

Discussion and Limitations

Discussion and limitationsThe method relies on strong dissipation to make the attractor finite-dimensional. Without dissipation, as in Hamiltonian or nearly conservative systems, the arguments above guarantee nothing. The rigorous conditions also give very conservative estimates of μ and h compared with what simulations show, and some cases, such as strongly chaotic Ginzburg–Landau regimes, still lack complete proofs.

The experiments also show practical sensitivities: the observation density must be adequate (Experiment 1), noisy data limit the accuracy that can be reached, and a very large μ makes the equations stiff.

Conclusion

In the three models, dissipation makes the information needed to synchronize a distributed chaotic system finite: large-scale modes, or measurements at points spaced by h, together with a coupling of strength μ. In the two experiments the error decays exponentially whenever the observations are dense enough and fails to decay when they are too sparse. The mathematical situation differs from model to model: the theory is complete for 2D Navier–Stokes, partial for Kuramoto–Sivashinsky and mainly numerical for Ginzburg–Landau. Open directions include sharper threshold estimates, three-dimensional systems, and the combination of coupling with unknown measurement noise.

References

[1] A. Azouani, E. Olson, E. S. Titi, Continuous data assimilation using general interpolant observables, J. Nonlinear Sci. 24, 277 (2014).

[2] A. Pikovsky, M. Rosenblum, J. Kurths, Synchronization: A Universal Concept in Nonlinear Sciences, Cambridge University Press (2001).

[3] C. Foias, G. Prodi, Sur le comportement global des solutions non stationnaires des équations de Navier–Stokes en dimension 2, Rend. Sem. Mat. Univ. Padova 39 (1967).

[4] E. Olson, E. S. Titi, Determining modes for continuous data assimilation in 2D turbulence, J. Stat. Phys. 113, 799 (2003).

[5] G. Pérez, H. A. Cerdeira, Extracting messages masked by chaos, Phys. Rev. Lett. 74, 1970 (1995).

[6] H. Bessaih, E. Olson, E. S. Titi, Continuous data assimilation with stochastically noisy data, Nonlinearity 28, 729 (2015).

[7] K. Hayden, E. Olson, E. S. Titi, Discrete data assimilation in the Lorenz and 2D Navier–Stokes equations, Physica D 240, 1416 (2011).

[8] K. M. Cuomo, A. V. Oppenheim, Circuit implementation of synchronized chaos with applications to communications, Phys. Rev. Lett. 71, 65 (1993).

[9] L. Junge, U. Parlitz, Synchronization and control of coupled Ginzburg–Landau and Kuramoto–Sivashinsky equations using spatially localized coupling, Phys. Rev. E 61, 3736 (2000).

[10] L. Kocarev, U. Parlitz, Generalized synchronization, predictability, and equivalence of unidirectionally coupled dynamical systems, Phys. Rev. Lett. 76, 1816 (1996).

[11] L. Kocarev, Z. Tasev, U. Parlitz, Synchronizing spatiotemporal chaos of partial differential equations, Phys. Rev. Lett. 79, 51 (1997).

[12] L. M. Pecora, T. L. Carroll, Synchronization in chaotic systems, Phys. Rev. Lett. 64, 821 (1990).

[13] L. M. Pecora, T. L. Carroll, Driving systems with chaotic signals, Phys. Rev. A 44, 2374 (1991).

[14] M. Altaf, E. S. Titi, O. M. Knio, L. Zhao, M. McCabe, I. Hoteit, Downscaling the 2D Bénard convection equations using continuous data assimilation, Comput. Geosci. 21, 393 (2017).

[15] M. Gesho, E. Olson, E. S. Titi, A computational study of a data assimilation algorithm for the two-dimensional Navier–Stokes equations, Commun. Comput. Phys. 19, 1094 (2016).